Journal of Geosciences and Geomatics, 2018, Vol. 6, No. 2, 65-76
Available online at http://pubs.sciepub.com/jgg/6/2/4
©Science and Education Publishing
DOI:10.12691/jgg-6-2-4

Contrasting Ba-Sr Granitoids from Bamenda Area, NW Cameroon: Sources Characteristics and Implications for the Evolution of the Pan African Fold Belt

Gus Djibril KOUANKAP NONO[1,*], Pierre WOTCHOKO[1], Alice MAGHA[1], Sylvestre GANNO[2], Ndam NJOYA[1], Aloysius AFAHNWIE NGAMBU[3], Jean Paul NZENTI[2], Veronique KAMGANG KABEYENE[2]

[1]Department of Geology, HTTC, University of Bamenda, P.O.Box 39 Bambili, Bamenda, Cameroon
[2]Department of Earth Sciences, Faculty of Sciences, University of Yaoundé 1, P.O.Box 812, Yaoundé, Cameroon
[3]Department of Geology, University of Buea, P.O.Box 63 Buea, Cameroon
*Corresponding author: kouankap@yahoo.fr

Received June 27, 2018; Revised August 03, 2018; Accepted August 13, 2018

Abstract The basement rocks of Bamenda town are mainly covered by volcanic rocks and are made up of two distinct types of granitoids: granites and leucogranites. These basement rocks belong geochemically to the same granite field. The studied granitoids are silica rich, with concentrations ranging from 70 to 73% in granite and 73 to 76% in leucogranite. Both belong to high-K calc-alcaline series with granite being magnesian and more potassic ($Na_2O/K_2O < 1$) whereas the leucogranite is ferriferous and similar to Na-granitoids ($Na_2O/K_2O >1$). Leucogranites are low Ba-Sr granitoids, strongly peraluminous (A/CNK > 1.1) and plot in the field of S-type granites, while granites are high Ba-Sr granitoids, slightly peraluminous and plot in the field of I-type granitoids. The chondrite-normalized REE patterns show more LREE enrichment in granites (>100*chondrite) than in leucogranites (>10*chondrite). Major and trace element compositions of the leucogranites and granites indicate crustal derivation from the partial melting of metapelite and metagreywacke respectively. The REE patterns display pronounced negative Eu anomalies (Eu/Eu* = 0.23-0.36) in leucogranites due to low degree of partial melting of a plagioclase depleted crustal source, and weakly negative to null Eu anomalies (Eu/Eu* = 0.81-1.08) in granites due to high degree of partial melting. The estimated temperatures of Bamenda granitoids magma range between 800°C and 950°C. Bamenda I-type granites are syn-tectonic and are similar to the other granitoids of the central domain of the Pan-African North-Equatorial Fold belt in Cameroon. Bamenda S-type peraluminous leucogranites are post-tectonic and chemically similar to the Himalayan peraluminous leucogranites. Furthermore, decompression model may be related to Bamenda leucogranite formation. Tectonically, the studied granitoids are related to crustal delamination characterizing the post-collisional event within the Pan African Fold Belt.

Keywords: *granites, High-K calc-alcaline series, peraluminous, metaluminous, crustal source, bamenda*

Cite This Article: Gus Djibril KOUANKAP NONO, Pierre WOTCHOKO, Alice MAGHA, Sylvestre GANNO, Ndam NJOYA, Aloysius AFAHNWIE NGAMBU, Jean Paul NZENTI, and Veronique KAMGANG KABEYENE, "Contrasting Ba-Sr Granitoids from Bamenda Area, NW Cameroon: Sources Characteristics and Implications for the Evolution of the Pan African Fold Belt." *Journal of Geosciences and Geomatics*, vol. 6, no. 2 (2018): 65-76. doi: 10.12691/jgg-6-2-4.

1. Introduction

Bamenda town is located at the foot of Mount Bamenda, which is part of the Cameroon Volcanic Line (CVL). CVL is a unique example on Earth of an active intra plate alkaline tectonic magmatic alignment simultaneously developed into both oceanic and continental domains [1]. Mount Bamenda to which belongs the study area is the fourth largest massif in volume in the continental sector of the plutonic-volcanic Cameroon line [2]. It consists of volcanic rocks (alkali basalt, trachyte, rhyolite, and ignimbrite) with age ranging from 22 Ma to present [3] and granito-gneissic basement of Pan-African ages [4,5]. Bamenda area is almost covered by volcanic products which have been studied in detail (eg., [2,3,6]) while the basement rocks remain poorly surveyed, probably because of the scarcity of outcrops. However, in a few places the granitic basement outcrops as windows in the volcanic cover enabling their observation and study. The available data on the Bamenda basement is restricted to the petrogenesis of peraluminous magma from Akum massifs, located about 12 miles to the south of Bamenda town [5]. Therefore, this piece of scientific research is a contribution to the geology of Bamenda basement, as it provides the first petrochemical characterization of two Contrasting Ba-Sr granitoids from Bamenda town.

2. Geological Setting

The basement rocks of Bamenda area belong to the central domain of the Pan-African Orogen formations in Cameroon (Figure 1a) also known as Pan-African North Equatorial Fold Belt (PANEFB). The PANEFB is a major Neoproterozoic orogen linked to the Trans-Saharan Belt of western Africa and to the Brasiliano Orogen of NE Brazil. In Cameroon, the PANEFB is made up of three geodynamic domains namely the southern, the central and the northern domains [4,7,8]. The study area belongs to the western part of the central domain (Figure 1) which is situated between the Sanaga fault to the south and the Tibati-Banyo fault to the north and characterized by syn-to post-tectonic granitoid intrusions related to regional large strike slip faults. These large NE-striking transcurrent faults, as well as the Adamaoua fault inside the central domain, are the prolongations of the major shear zones of NE Brazil in a pre-drift Gondwana reconstruction [9,10]. The central domain of the PANEFB consists of an assembly of fragments of Paleoproterozoic continental crust recrystallised under high-grade granulite facies (850-900°C, 10-12Kb) at ca 2100Ma [11] intruded by widespread Neoproterozoic plutonic rocks of high-K, calc-alkaline affinities [12,13,14,15,16]. [5] in Akum area located south of the study area have distinguished a rock sequence consisting of peraluminous S-type leucogranites and orthogneissified I-type biotite granite (Figure 1b); all displaying characteristics of medium to high-K calc-alkaline series.

3. Analytical Methods

Standard thin sections were prepared from representative dozen of fresh samples at Geotech Lab (Vancouver, Canada) using conventional techniques. Mineral identification was attained by petrographic studies under both polarized and plane polarized light at the Geology Laboratory of the University of Bamenda (Cameroon).

Whole-rock analyses for major elements were done by Inductively Coupled Plasma-Atomic Emission Spectroscopy (ICP-AES) using the pulp at ALS (Australian Laboratory Services), Vancouver (Canada), on thirteen carefully selected granitoid samples. A prepared sample (0.200 g) was added to lithium metaborate/lithium tetraborate flux (0.90 g), well mixed and fused in a furnace at 1000°C. The resulting melt was then cooled and dissolved in 100mL of 4% nitric acid and 2% hydrochloric acid. This solution was then analyzed by ICP-AES and the results were corrected for spectral inter-element interferences. Oxide concentration was calculated from the determined elemental concentration and the result was reported in that format. Trace element concentrations were determined by Inductively Coupled Plasma–Mass Spectroscopy (ICP-MS). A prepared sample (0.200 g) was added to lithium borate flux (0.90 g), well mixed and fused in a furnace at 1000°C. The resulting melt was then cooled and dissolved in 100 mL of 4% HNO_3 and 2% HCl solution. Analytical uncertainties vary from 0.1 % to 0.04 % for major elements; 0.1 to 0.5% for trace elements; and 0.01 to 0.5 ppm for rare earth elements.

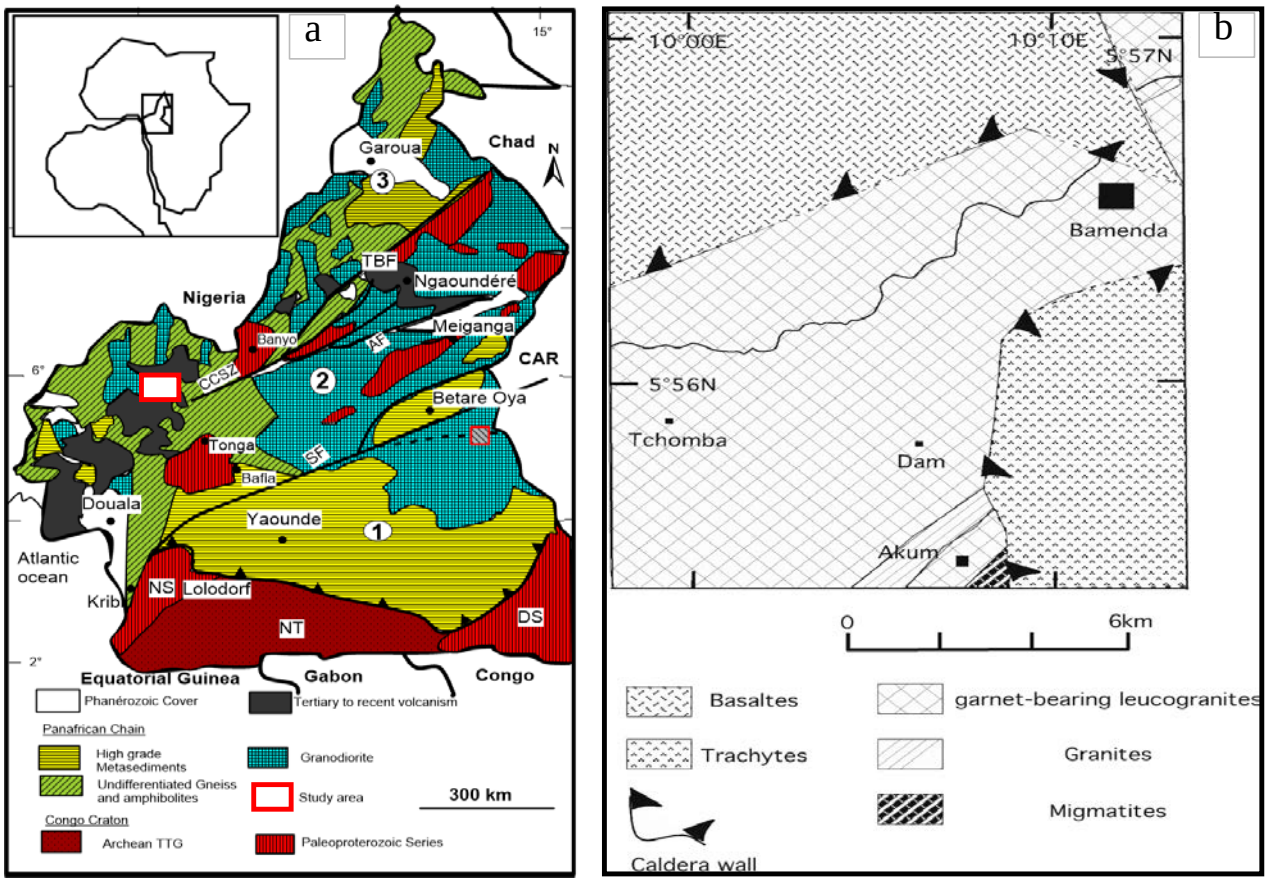

Figure 1: **a)** Geological map of Cameroon with the three main domains of the Pan-African North-Equatorial fold belt (modified from [5]: (1) southern domain corresponding to the Yaoundé series thrust on the Congo Craton, (2) central domain, (3) northern domain. TBF, Tibati-Banyo Fault; CCSZ, Central Cameroon Shear Zone; SF, Sanaga Fault; ASZ, Adamaoua Shear Zone; NT, Ntem complex; DS, Dja series; NS, Nyong series. Bamenda area is marked by a white rectangle **b)** Geological map of the Akum-Bamenda Massif [5] showing the location of Bamenda town (Black filled square)

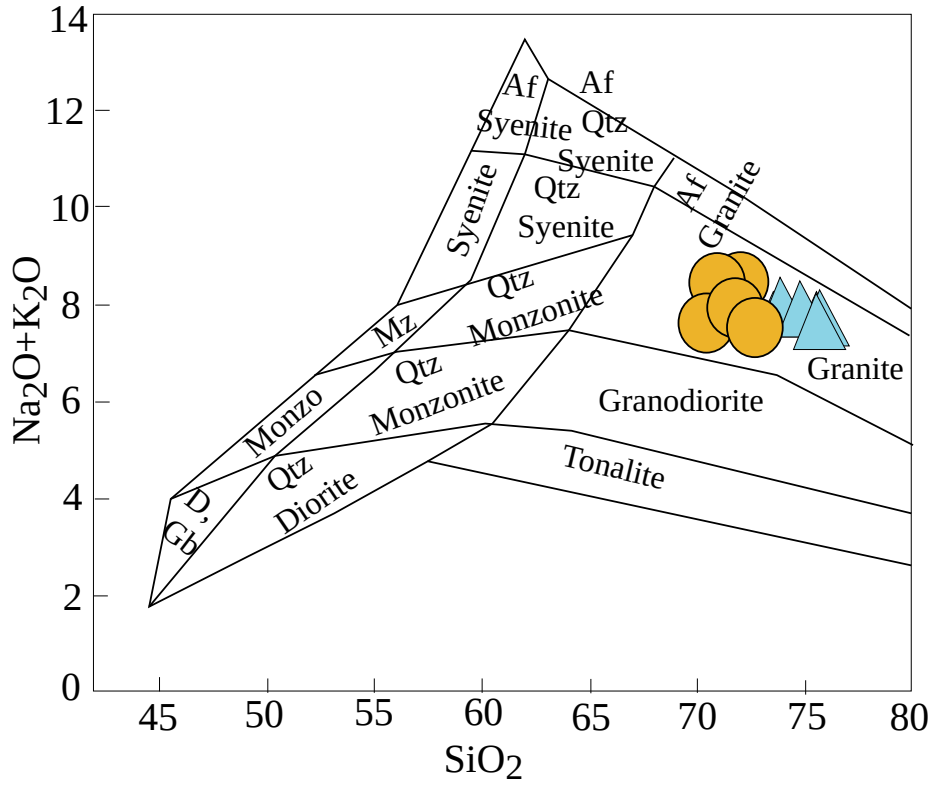

Figure 2. TAS diagram of [17], showing the position of the studied samples within the granite domain (Granite ●, Leucogranite ▲)

4. Results

4.1. Rock Classification and Petrography

In the classification diagram of Total Alkali versus Silica of [17], all the samples plot in the granite field (Figure 2). However, based on the color of fresh samples and the relative abundance of minerals, the studied samples have been separated into two groups corresponding to two different rock types: leucogranite for the leucocratic or light group and granite for the mesocratic or light grey group.

4.1.1. Leucogranites

Leucogranites outcrop as metric size boulders and as flagstones. The fresh samples show light color with some dark marks (Figure 3A & Figure 3B). The thin section studies indicate a granular porphyritic microstructure (Figure 3C & Figure 3D) with the main minerals being quartz (50-60 vol.%), plagioclase (20-25 vol.%), K-feldspar (10-15 vol.%), micas (05-10 vol.%) and opaque minerals (01–05 vol.%). Quartz is the main mineral in the rocks and shows subhedral to anhedral crystals, commonly in association with plagioclase. Plagioclase displays different forms and sizes. The larger crystals are euhedral, and contain inclusions of opaque minerals. Some of the large plagioclase crystals are fractured and these cracks are filled by fine grains of quartz. Mica crystals are anhedral (mica flakes) and contain inclusions of opaque minerals.

4.1.2. Granites

Granites outcrop as boulders of various dimensions; they are medium grained and light grey in color (Figure 3E & Figure 3F). Under the microscope, the rocks display a heterogranular microstructure (Figure 3G & Figure 3H) with modal composition made up of K-feldspar (20-30 vol.%), quartz (15-25 vol.%), plagioclase (10-20 vol.%), biotite (15-20 vol.%), amphibole (05-10 vol.%) and opaque minerals (01-05 vol.%). Quartz yields two habits phenocrysts which are anhedral with undulatory extinction and small crystals which are subhedral generally associated with K-feldspars. K-feldpar present here is large xenomorphic crystals of orthoclase exhibiting various sizes. Plagioclase intergrows in some place with quartz to form myrmekites (Figure 3G). Amphibole is green hornblende, with the elongated shape crystals which in some samples, underwent transformation to biotite.

4.2. Geochemistry

4.2.1. Major Elements

The whole rock geochemical data of granites and leucogranites are presented in Table 1. Both rocks are rich in silica. Leucogranites have the highest SiO_2 content, ranging from 73 to 76%., whereas the silica content of granites varies from 70 to 73%. The Harker diagrams (Figure 4) reveal well pronounced negative and positive correlations. Al_2O_3, Na_2O and MnO concentrations exhibit a positive correlation with SiO_2; whereas Fe_2O_3, MgO, CaO, K_2O and P_2O_5 exhibit a negative correlation with SiO_2.

P_2O_5 and TiO_2 concentrations in both rocks are low (0.08% and 0.2%). This is probably related to the fractional crystallization of apatite and titanite. The high-K Calc-alkaline affinity of the studied Bamenda granitoids can be depicted from the SiO_2 vs K_2O diagram of [18], where the studied granites and leucogranites belong to high-K calc-alkaline series with one sample of leucogranites plotting within the calc-alkaline series field (Figure 5).

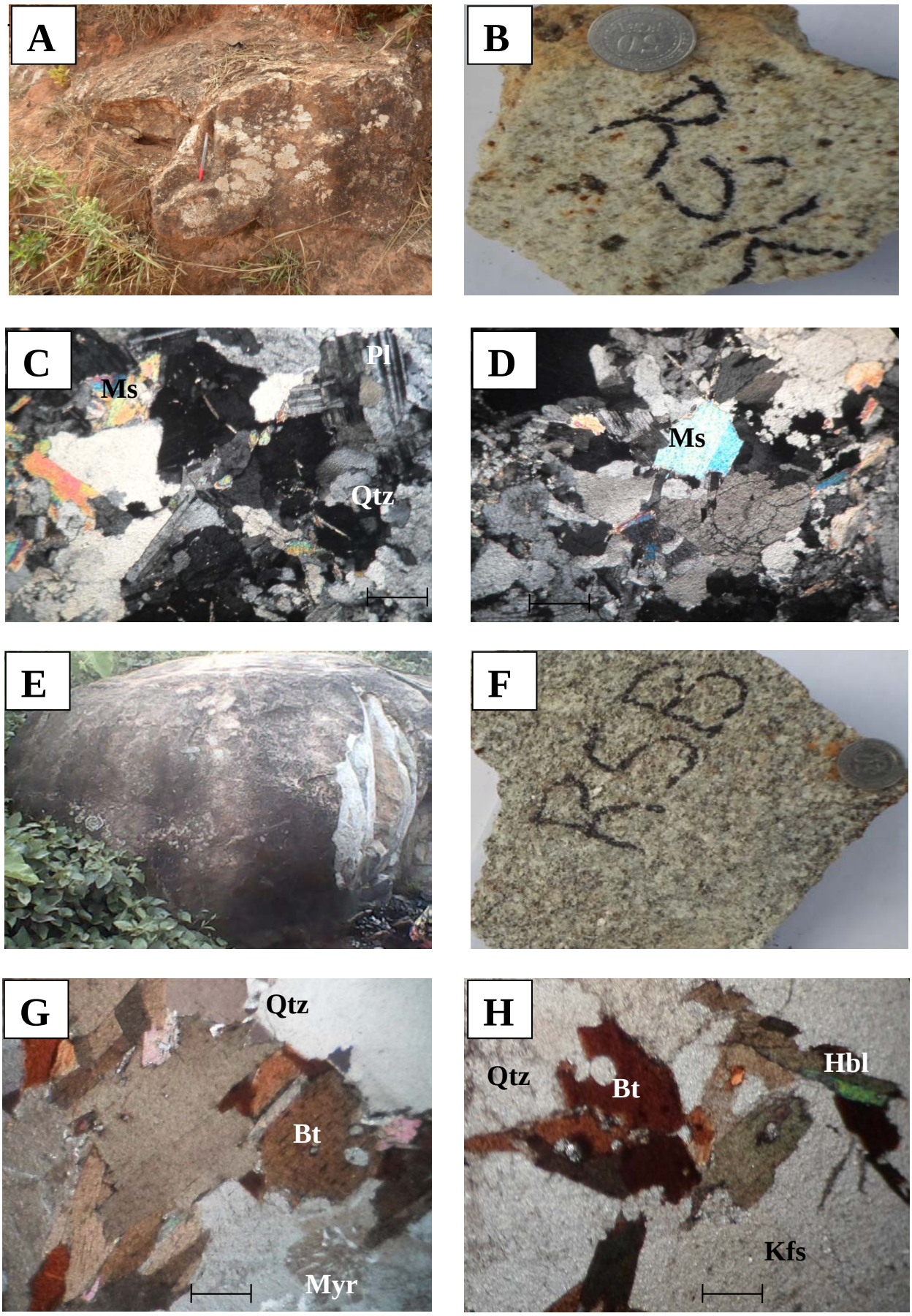

Figure 3. Photographs and photomicrographs (scale bar = 0.1 mm) of the granitoids from Bamenda town. *Leucogranites*: outcrop picture (A) and hand specimen sample (B), C and D are photomicrographs displaying the mineral composition and microstructure. *Granites*: outcrop (C) and hand specimen sample (D) views; G and H are photomicrographs displaying microstructure and mineral assemblage

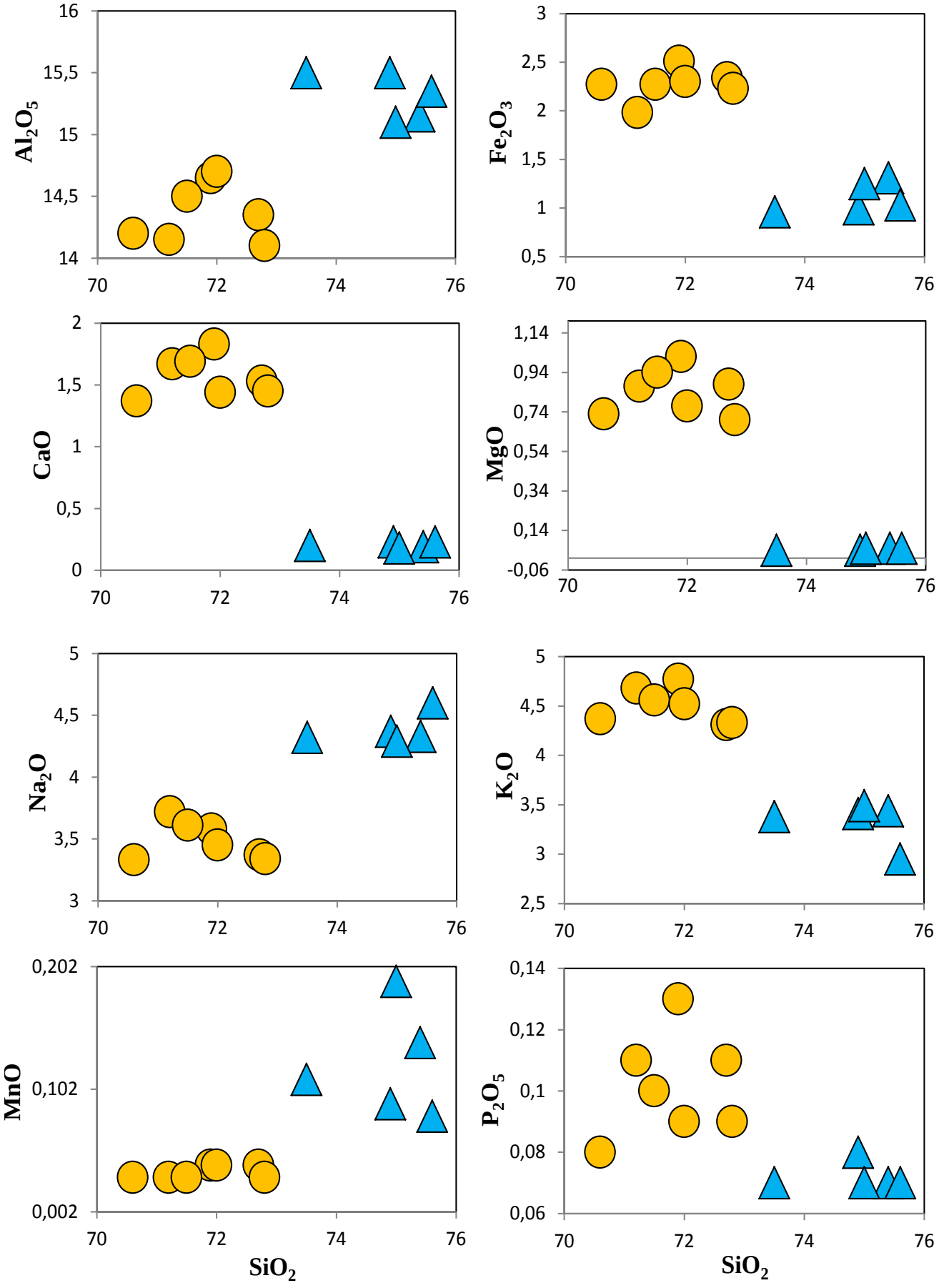

Figure 4. Harker diagrams showing variation of major elements versus silica. (Granite ●, Leucogranite ▲)

Table 1. Major (wt%) and trace (ppm) elements of leucogranites and granites from Bamenda town

Rock	LEUCOGRANITE					GRANITE						
Code	**RSK1**	**RSK2**	**RSK3**	**RSK4**	**RSK5**	**RSB1**	**RSB2**	**RSB4**	**RSB5**	**RSB6**	**RSB7**	**RSB8**
SiO_2	75.4	73.5	74.9	75.6	75	71.9	71.2	70.6	72.7	71.5	72.8	72
Al_2O_3	15.15	15.5	15.5	15.35	15.1	14.65	14.15	14.2	14.35	14.5	14.1	14.7
Fe_2O_3	1.31	0.96	0.99	1.03	1.25	2.51	1.98	2.27	2.34	2.27	2.23	2.3
CaO	0.19	0.2	0.23	0.23	0.18	1.83	1.67	1.37	1.53	1.69	1.45	1.44
MgO	0.05	0.04	0.04	0.05	0.05	1.02	0.87	0.73	0.88	0.94	0.7	0.77
Na_2O	4.33	4.32	4.37	4.6	4.29	3.58	3.72	3.33	3.37	3.61	3.34	3.45
K_2O	3.44	3.38	3.41	2.95	3.49	4.77	4.68	4.37	4.31	4.56	4.33	4.52
Cr_2O_3	<0.01	<0.01	<0.01	<0.01	<0.01	0.01	<0.01	<0.01	0.01	<0.01	<0.01	<0.01
TiO_2	0.01	0.01	0.01	0.01	0.01	0.38	0.31	0.27	0.33	0.33	0.27	0.29
MnO	0.14	0.11	0.09	0.08	0.19	0.04	0.03	0.03	0.04	0.03	0.03	0.04
P_2O_5	0.07	0.07	0.08	0.07	0.07	0.13	0.11	0.08	0.11	0.1	0.09	0.09
SrO	<0.01	<0.01	<0.01	<0.01	<0.01	0.17	0.17	0.14	0.14	0.17	0.14	0.15
BaO	<0.01	<0.01	<0.01	<0.01	<0.01	0.3	0.27	0.22	0.23	0.27	0.23	0.23
LOI	1.53	1.86	1.64	1.94	1.8	0.62	0.64	0.61	0.72	0.79	0.53	0.56
Total	**101.62**	**99.95**	**101.26**	**101.91**	**101.43**	**101.91**	**99.8**	**98.22**	**101.06**	**100.76**	**100.24**	**100.54**
Na_2O+K_2O	**7.77**	**7.7**	**7.78**	**7.55**	**7.78**	**8.35**	**8.4**	**7.7**	**7.68**	**8.17**	**7.67**	**7.97**
Na_2O/K_2O	**1.26**	**1.28**	**1.28**	**1.55**	**1.23**	**0.75**	**0.79**	**0.76**	**0.78**	**0.79**	**0.77**	**0.76**
A/NK	**1.25**	**1.29**	**1.28**	**1.30**	**1.25**	**1.14**	**1.10**	**1.20**	**1.22**	**1.16**	**1.20**	**1.20**
A/CNK	**1.22**	**1.25**	**1.23**	**1.25**	**1.21**	**0.91**	**0.89**	**0.99**	**0.98**	**0.93**	**0.98**	**0.99**
Ba	18.6	7.5	8.2	9.8	23.5	2670	2430	2060	2120	2510	2170	2120
Ce	4.4	4.1	4.8	5.3	5	112.5	94.6	81.9	94.3	98.3	89	96.2
Cr	10	10	10	10	10	40	30	30	30	40	30	30
Cs	9.19	9.07	8.85	7.37	9.04	3.36	3.14	2.88	3.1	3.99	2.78	2.9
Dy	0.94	0.83	0.82	0.75	1.09	2.39	2.21	1.35	1.68	2.16	1.6	1.55
Er	0.42	0.39	0.41	0.31	0.46	1.24	0.94	0.6	0.9	1.03	0.81	0.77
Eu	0.09	0.1	0.13	0.07	0.1	1.27	1.24	1.09	1.08	1.28	1.16	1.03
Ga	38.4	38.7	37.2	35.5	36.9	21.2	18.7	17.7	18.8	19.5	17.8	18
Gd	0.83	0.81	0.92	0.74	0.83	3.7	3.02	2.23	2.79	3.43	2.49	2.63
Hf	2.6	2.2	2.3	2.3	2.7	6.1	5.6	3.9	4.6	5.1	4.5	4.3
La	4.7	4.6	6.8	3.5	5.6	62.4	52.7	45.3	51.5	53	48.3	52.3
Lu	0.07	0.08	0.07	0.07	0.08	0.17	0.15	0.1	0.14	0.15	0.12	0.13
Nb	34	44.5	36	26.5	38.8	12.8	11.5	8.9	10.6	12	9.6	9.8
Nd	3.7	4	5.3	3.1	4.6	42.9	35.3	28.7	33.4	35.9	31	33.4
Pr	1.11	1.18	1.55	0.89	1.33	12.05	10.5	8.6	9.94	10.6	9.45	10.15
Rb	370	362	365	303	365	109	99.1	87.9	90.5	104.5	84.5	88.8
Sm	0.99	0.97	1.29	1.08	1.08	6.18	5.29	4.2	4.81	5.73	4.45	5.04
Sn	34	34	33	27	31	2	2	2	2	3	2	2
Sr	8.4	5.1	5.3	5.6	5.3	1470	1360	1220	1245	1420	1260	1240
Ta	4	7.7	4.9	2.6	8.2	1.3	1.3	0.7	0.8	1.1	0.8	0.8
Tb	0.16	0.13	0.17	0.13	0.19	0.46	0.41	0.27	0.34	0.42	0.3	0.3
Th	1.43	1.14	1.11	1.81	2.22	13.9	13.15	12.25	12.95	16.85	12.75	13.9
U	3.12	2.56	2.62	3.47	3.48	2.93	4.19	2.99	2.95	10.45	5.78	4.68
V	<5	<5	<5	<5	<5	24	20	19	22	23	18	19
Yb	0.47	0.54	0.44	0.49	0.52	1.29	1.06	0.67	0.74	0.88	0.79	0.73
Y	5.4	4.4	4.2	3.8	6.2	11.8	10.7	6.9	9.1	10.9	8.1	8
Zr	33	31	32	32	37	222	195	156	188	201	176	172
Bi	1.56	1.49	4.43	7.84	1.95	0.32	0.84	0.13	0.14	0.87	0.17	0.11
Co	1	2	1	2	1	4	4	4	4	4	3	4
Cu	<1	1	1	1	1	11	10	10	13	17	12	11
Li	60	60	50	50	50	30	30	30	40	30	30	30
Ni	1	1	<1	<1	1	19	16	14	17	17	16	15
Pb	12	12	11	13	15	57	60	57	54	60	57	54
Zn	21	22	22	20	18	47	43	39	48	46	40	42
∑REE	**18.13**	**17.93**	**22.92**	**16.62**	**21.15**	**247.17**	**207.96**	**175.34**	**202.09**	**213.4**	**189.89**	**204.63**
(Ce/Sm)N	**1.07**	**1.02**	**0.90**	**1.18**	**1.12**	**4.39**	**4.31**	**4.71**	**4.73**	**4.14**	**4.83**	**4.61**
(La/Yb)N	**6.75**	**5.75**	**10.43**	**4.82**	**7.27**	**32.65**	**33.56**	**45.63**	**46.97**	**40.65**	**41.27**	**48.36**
(Gd/Yb)N	**1.43**	**1.21**	**1.69**	**1.22**	**1.29**	**2.32**	**2.30**	**2.69**	**3.04**	**3.15**	**2.55**	**2.91**
(Gd*Sm)N	**26.12**	**24.97**	**37.72**	**25.40**	**28.49**	**726.77**	**507.77**	**297.69**	**426.54**	**624.68**	**352.18**	**421.31**
(La/Lu)N	**6.97**	**5.97**	**10.08**	**5.19**	**7.26**	**38.10**	**36.46**	**47.02**	**38.18**	**36.67**	**41.78**	**41.76**
(La/Sm)N	**2.99**	**2.98**	**3.32**	**2.04**	**3.26**	**6.36**	**6.27**	**6.79**	**6.74**	**5.82**	**6.83**	**6.53**
(Gd/Lu)N	**1.47**	**1.26**	**1.63**	**1.31**	**1.29**	**2.70**	**2.50**	**2.77**	**2.47**	**2.846**	**2.58**	**2.51**
Eu/Eu*	**0.30**	**0.34**	**0.36**	**0.24**	**0.33**	**0.81**	**0.95**	**1.08**	**0.90**	**0.88**	**1.06**	**0.86**

Note: A/NK=$Al_2O_3/(Na_2O+K_2O)$ and A/CNK=$Al_2O_3/(CaO+Na_2O+K_2O)$, molar ratio (1000 * wt% / Molecule mass).

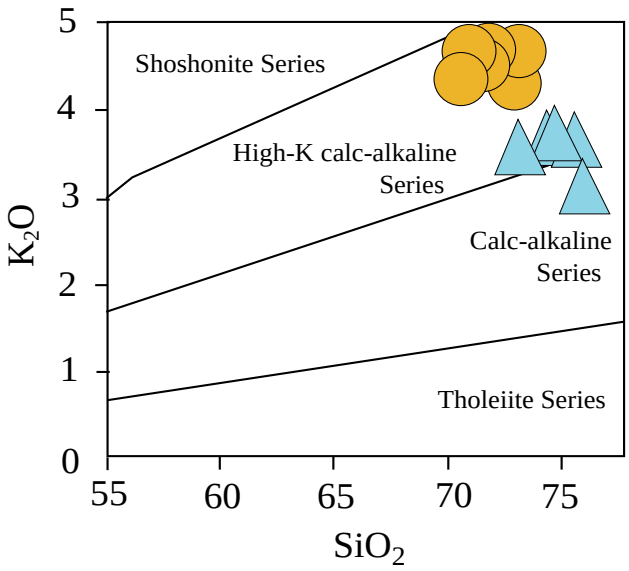

Figure 5. K_2O vs SiO_2 diagram of [18] showing the calc-alkaline to high K- calc-alkaline affinities of granites and leucogranites from Bamenda (Granite ●, Leucogranite ▲)

The sum of alkaline elements (Na_2O+K_2O) is relatively constant and high, ranging from 7.55 to 7.78% in leucogranites and from 7.67 to 8.35% in granites. The major contrast between the studied leucogranites and granites is their alkali content. Granites are more enriched in K_2O than leucogranites. The Na_2O/K_2O versus SiO_2 diagram of [19] defining Na-granitoids and K-granitoids reveals that leucogranites are Na-granitoids whereas granites are K-granitoids (Figure 6).

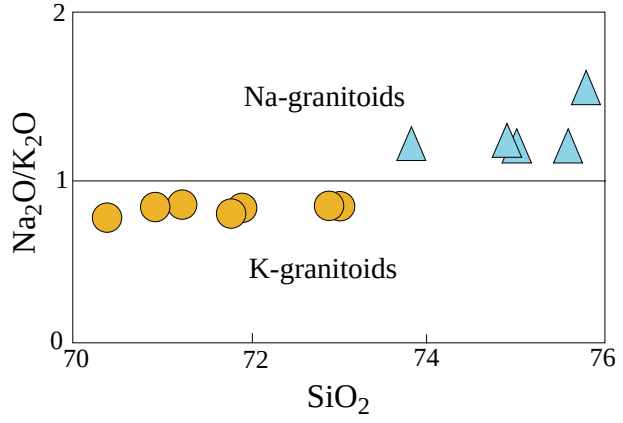

Figure 6. Na_2O/K_2O versus SiO_2 defining Na-granitoids field and K-granitoids field after [19] (Granite ●, Leucogranite ▲)

The granites are also richer in calcium than leucogranites. In the diagram TiO_2 vs Zr (Figure 7a) of [20]. all the leucogranites plot in the domain of S-granitoid, while granite samples plot in the I-granitoid domain. In the Aluminium Saturation Index diagram A/CNK-A/NK of [21], all studied samples are peraluminous with leucogranites being more peraluminous (Figure 7b).

Granites have a high mafic content (Fe_2O_3 + MgO + TiO_2 = 3.16 to 3.91%) compared to the leucogranites (Fe_2O_3 + MgO + TiO_2 = 1.01 to 1.37%). The classification diagram of [22] discriminating ferroan granitoids and magnesian granitoids, reveals the magnesian and ferriferous characters for granite and leucogranites respectively (Figure 8a). The millications Fe+Mg+TivsMg/Mg+Fe diagram of the same author confirm these geochemical characters, with granites plotting in the field of magnesian series and leucogranites plotting in the field of ferriferous series (Figure 8b).

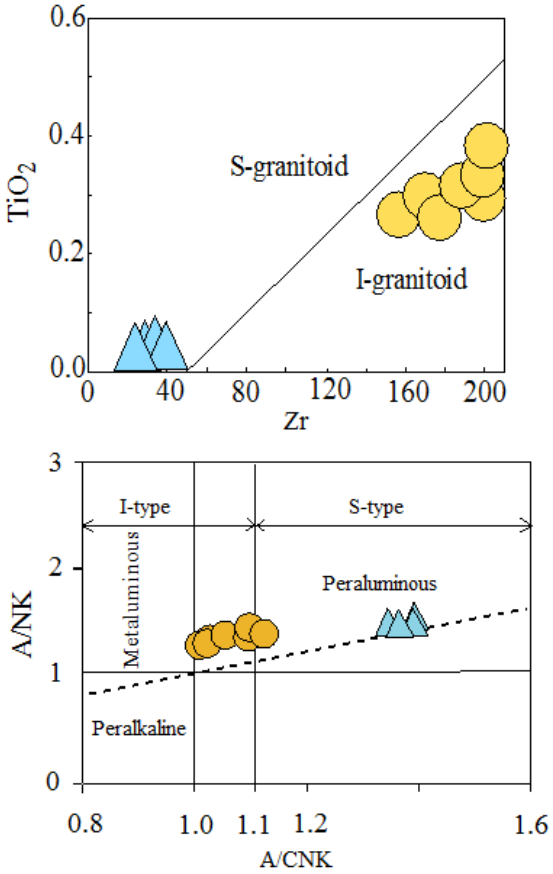

Figure 7. a) TiO_2 vs Zr diagram discriminating Bamenda granitoids into I- and S-type. b) Alumina index diagram A/CNK-A/NK for Bamenda town granitoids. Boundary between I-type and S-type granite is after [21]

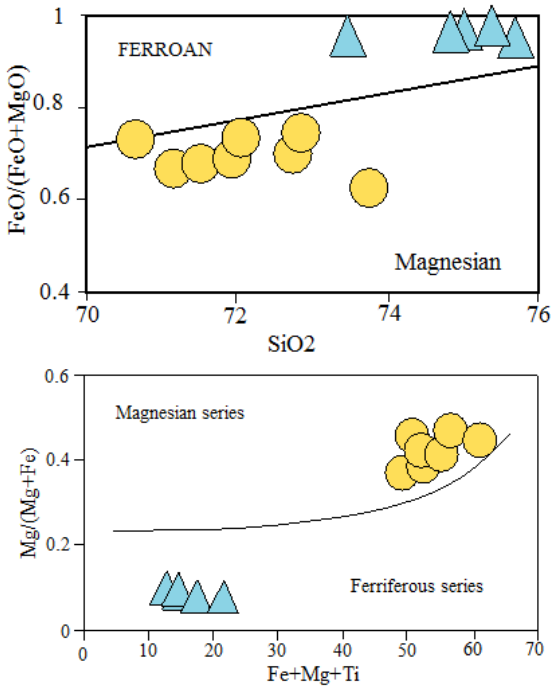

Figure 8. a) The SiO_2 vs FeOt/(FeOt + MgO) diagram, showing magnesian and ferriferous characteristics of the studied granitoids (axis units are wt%). b) Millications diagram Fe+Mg+Ti vs Mg /Mg+Fe defining magnesian and ferriferous series

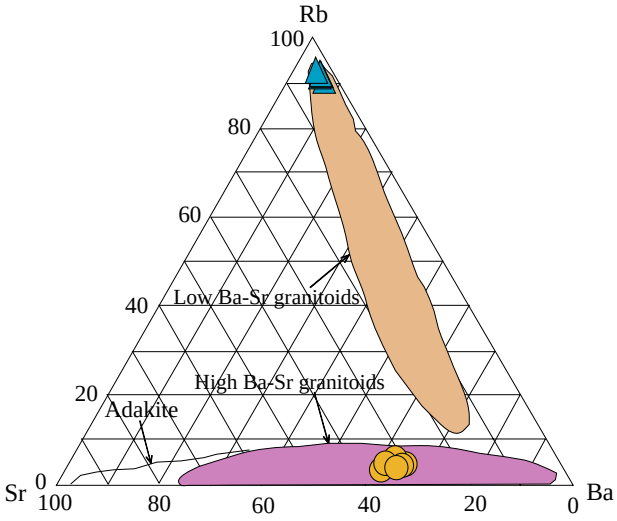

Figure 9. Sr-Rb-Ba plot for the Bamenda granitoids

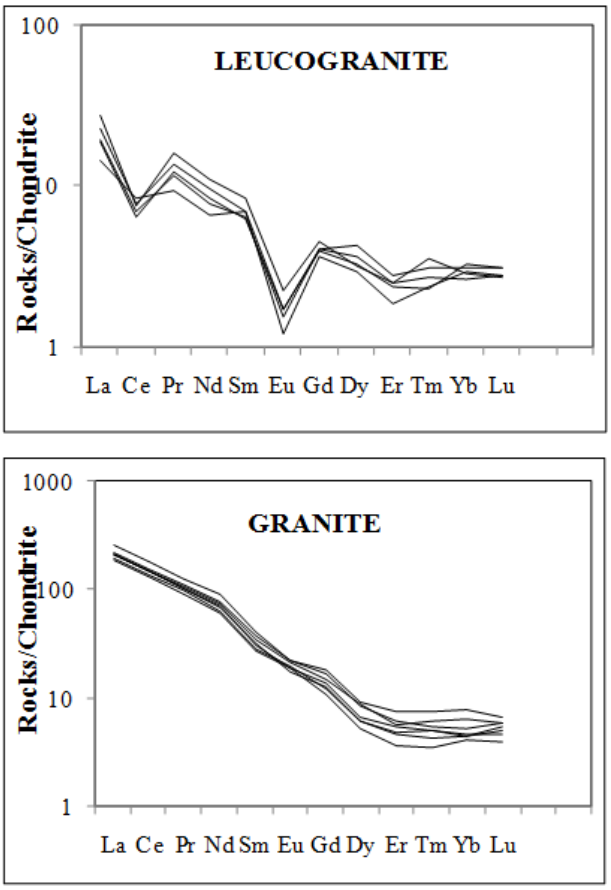

Figure 10. Chondrite-normalised REE patterns of leucogranites and granites from Bamenda town, normalizing values after [24]

4.2.2. Trace Elements, Including REE

The trace element data from whole rock geochemistry of granites and leucogranites are presented in Table 1. Rb concentrations are high (300-370 ppm) in leucogranites and comparatively low concentration in granites. The high Rb of leucogranites can be attributed to late feldspar crystallization. Ba contents is high in granites (2000-2700 ppm) and very low (7 - 24 ppm) in leucogranites. The variation of Ba concentration is controlled by the presence of K-feldspar and biotite. These minerals are scarce in leucogranites and abundant in granites. The Ba/Rb ratios are very low in the leucogranites and ranging between 0.02 and 0.06. In the granites these ratios are relatively high (23.43-25.68) compared to the values observed in continental calc-alkaline igneous granitoids in Mali, West Africa [23]. Regarding the Ba/Sr ratios, granites and leucogranites yield values within the same ranges from 1.4 to 2.2 with sample RSK5 of leucogranites having 4.434. Sr-Rb-Ba plot of the Bamenda granitoids yields a clear distinction between the studied rocks (Figure 9), leucogranites are low Ba-Sr granitoids while granites are high Ba-Sr granitoids.

The chondrite-normalised rare earth element (REE) patterns (Figure 10) of the studied Bamenda rocks are quite different. Leucogranite patterns are more or less parallel, less fractionated, showing a weak LREE (light rare earth element) enrichment with La_N/Yb_N ratios < 11 and Gd_N/Yb_N ratios of 1.21–1.69. Leucogranites have negative Ce anomalies with strong negative Eu anomalies. Whereas, REE patterns of granites are quite parallel, showing high LREE enrichment (La_N/Yb_N ratios of 32.65-48.36 and Gd_N/Yb_N ratios of 2.30-3.15). Eu anomalies are variable in granites (Eu/Eu* = 0.81-1.08). When comparing the two rocks suites, the chondrite-normalized patterns show that granites have higher LREE concentrations (> 100*chondrite) than leucogranites (>10*chondrite). In contrast their HREE concentrations are similar in both granitoid types.

5. Discussion

5.1. Origin of Bamenda Granitoid Magma

The behavior of Bamenda granitoids on Harker diagrams does not indicate a continuous compositional variation, but clearly expresses two distinct groups, this reveals that the chemical differences of these granitoids seem to reflect the primary compositions of two distinct source rocks. High SiO_2, Al_2O_3 and low MgO coupled to the values of Ce/Pb ratios, which are far from the typical mantle values (Ce/Pb=25, [25]) suggest that the Bamenda granitoids are from crustal melt. The studied felsic rocks show weakly negative Eu anomalies which can be attributed to the high degree of partial melting [26], whereas the well pronounced negative Eu anomalies in leucogranites may be the results of low degree of partial melting where only the felsic components of source rocks melted leaving the mafic components as solid residus [27]. K-rich granites are generally derived from the partial melting of metamorphosed hydrous intermediate calc-alkaline rocks [28]. In the molar Al_2O_3/(MgO+FeOt) vs CaO/(MgO+FeOt) diagram (Figure 11a), the granites and leucogranites plot respectively in the fields of the partial melting of metagreywackes and metapelites. These features indicate that both groups of granitoids are from distinct sources and this fact highly clarifies their petrographical and geochemical differences. The LREE enrichment and HREE depletion behavior observed in Bamenda granitoids had also been noticed by [4] and interpreted as compatible with fractionation of amphibole which tends to concentrate the HREE. The high contents of LREE in leucogranites could be related to the enrichment of their source materials in LREE because Y and Yb show no

negative anomalies, suggesting that garnet was not involved in the residual phase (Figure 11b).

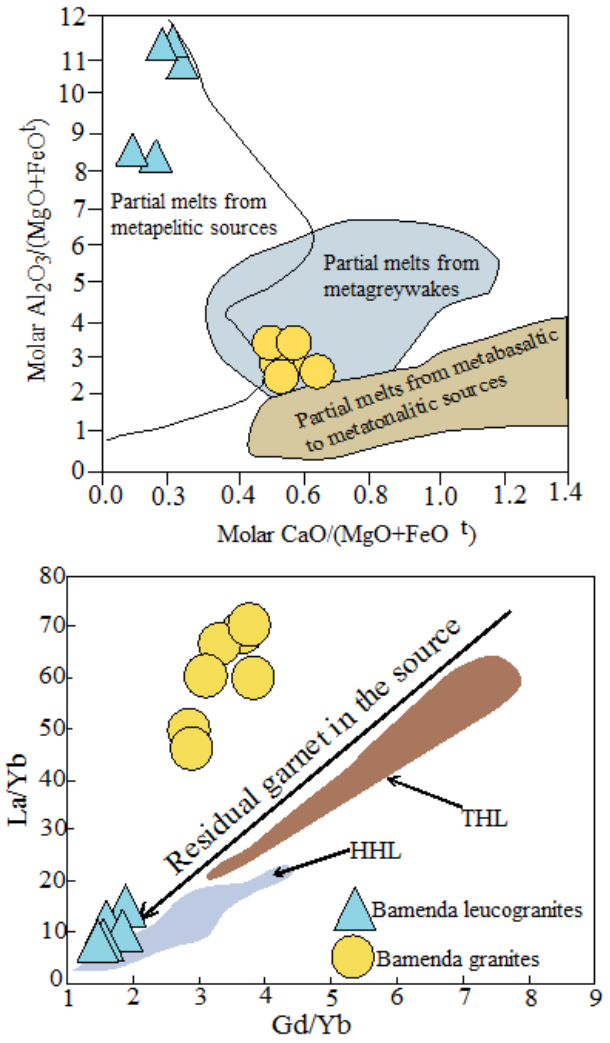

Figure 11. a) Molar diagram CaO/(MgO+FeOt) vs Al_2O_3/(MgO+FeOt) for the Bamenda granites. b) La/Yb vs Gd/Yb showing the trend of the residual garnet in the source and the positions of Bamenda granitoids and Himalayan leucogranites (HHL & THL).

The Eu anomalies go along with the plagioclase formation. Its variation (negative and positive) in Bamenda granitoids may indicate melting under low and high hydrous (H_2O) conditions respectively [29]. The well pronounced negative Eu anomalies in Bamenda leucogranites indicate a melting in low hydrous condition of low degree of partial melting of the continental crust and this is similar to some well-studied Himalayan leucogranites [30,31,32]. Bamenda granites are derived from high degree of partial melting of metagreywackes having a significant amount of hydrous minerals. This source of Bamenda granite is similar to the one of many granitic plutons studied in the central domains of the PANEFB in Cameroon [14] and within its prolongation in the NE Brazil. According to [4], negative anomalies of some trace elements result either from the low content of these elements in the source, or their retention in the residue during partial melting.

5.2. Crystallization Temperature

The crystallization temperature of the studied Bamenda granitoids was estimated by two different methods. The temperature for the high-K Calc-alkalic magma can be estimated using the whole rock P_2O_5 and SiO_2 contents [33]. According to these authors, there is a relationship between apatite saturation and the silica content of magma. The temperature can be also determined by using the diagram Zr (ppm) vs M=(Na+K+2Ca)/(Al*Si) of [34], based on the fact that zircon and apatite may resist complete dissolution during crustal partial melting, and therefore the amount of dissolved zirconium can be used to determine the temperature in the granitic melts. In the P_2O_5 vs SiO_2 binary diagram (Figure 12a) where dash lines represent isotherms at 7.5kb pressure, Bamenda granitoids display a trend between the 800°C and 950°C isotherms. Figure 12b shows temperatures of about 900°C for granites and about 800°C for leucogranites. These temperatures are close to the liquidus temperatures estimation proposed by [35]. This author has proposed a zirconium saturation thermometer using the equation T°(C) = -273 + 12,900/[17.18 – ln(Zr)]. The estimated crystallization temperatures are 800°C and 700°C for the studied Bamenda granites and leucogranites respectively.

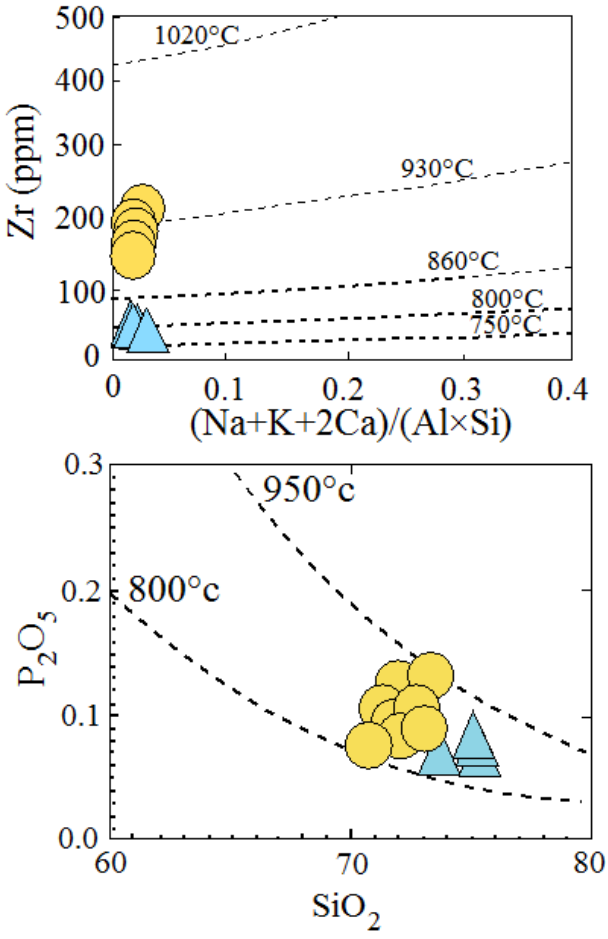

Figure 12. P_2O_5 vs SiO_2 (a) and Zr vs (Na+K+2Ca)/(Al*Si) (b) temperatures diagrams of Bamenda granitoids.

5.3. Tectonic Setting and Pan-African Fold Belt Evolution in Cameroon

The central domain of the PANEFB in Cameroon is marked by the Central Cameroon Shear Zone (CCSZ), which is a major tectonic structure in a transitional zone between the Congo Craton and a mobile zone [36,37,38]

and it is characterized by the delamination of the continental lithosphere [36]. In the millications R1 versus R2 discrimination diagram (Figure 13) of [39] used to distinguish the tectonic setting, Bamenda granites plot in the syn-collision field whereas Bamenda leucogranites plot in the post-tectonic field. From the two geotectonic settings proposed by [40] to constrain the generation of high-K and cal-alkaline magma, the syn- to post-collisional settings could be reasonably ascribed to Bamenda granitoids which is consistent regarding their comparison with other works carried out in the eastern part of the central domain of the Pan African Fold Belt in Cameroon [4,5,12,14]. According to [41], the crustal source rocks of high-K magmas in this context may occur as a consequence of decompression following the lithospheric root delamination. Based on the work of [42] the post collisional period is particularly known for producing magma from different sources. All these evidences indicate that the collision between the Congo Craton and the West African Craton was followed by a decompression phase associated with the crustal delamination which coupled to the CCSZ put in place the Bamenda granitoids. The geochemical similarities may lead us to assume that Bamenda leucogranites and the Himalayan leucogranite have the same geological model.

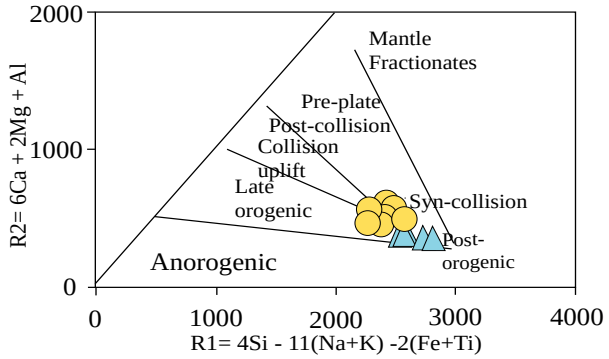

Figure 13. Millications diagram R1 versus R2 of [39] showing the position of granites in the syn-collision domain and the leucogranites in the post-orogenic domain

5.4. Comparison with Himalayan Leucogranites

The two studied granites present a close spatial field relationship and display different mineral content. Granites have higher proportions of mafic minerals than leucogranites. These major differences amongst the same rock types in the same geological setting may be either due to their sources or to different magmatic processes involved in their formations. Although the study of granitoids within the central domain of PANEFB has permitted to gather more information about magma generation, little is known concerning late- to post- tectonic leucogranites. Therefore, we carry a comparative study alongside discussion with some well documented Himalayan leucogranites to infer some related facts. The petrochemical characteristics of Bamenda leucogranites show many similarities with Himalayan leucogranites. For example, both leucogranites are peraluminous ([22]; Figure 14) and correspond to S-type granites.

The Ce/Pb versus Ce binary diagram (Figure 15) suggestss that the Bamenda granitoids are from continental crust, with granites being from Upper Continental Crust (UCC) and leucogranites from Lower Continental Crust (LCC). Furthermore, Himalayan leucogranites share the same source field with Bamenda leucogranites which is clearly distinct from Bamenda granite, providing further support to the hypothesis of two different sources for the studied granitoids.

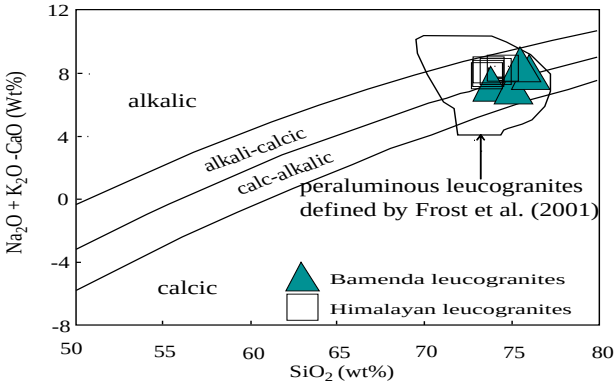

Figure 14. SiO_2 vs Na_2O+K_2O+CaO diagram showing the plot of the Bamenda leucogranites and Himalayan leucogranites in the peraluminous field defined by [22]. Data of Himalayan leucogranites after [31]

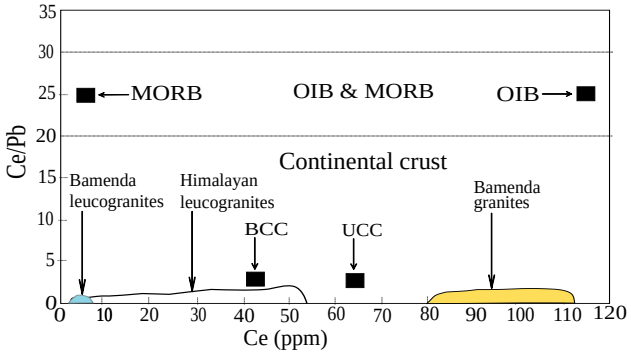

Figure 15. Ce/Pb versus Ce binary diagram discriminating sources of granitoids

The chondrite-normalized patterns of the representative Himalyan leucogranites are similar to those of Bamenda leucogranites (Figure 16), and show LREE enrichment and relative HREE depletion, with Himalayan leucogranites being slightly more depleted, similar to the pattern of the continental crust originated rocks. These patterns also show pronounced negative Eu anomalies, which indicate a plagioclase-depleted crustal source.

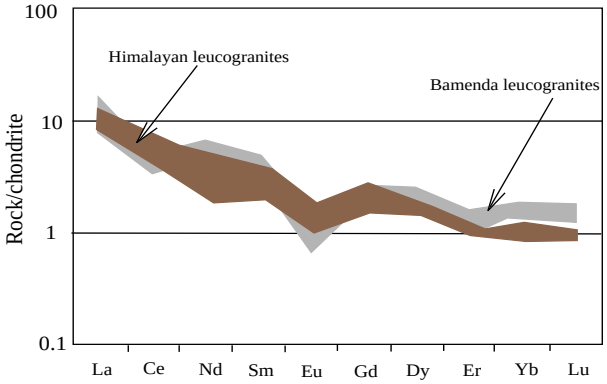

Figure 16. Comparative chondrite-normalized REE patterns of Himalayan leucogranites and Bamenda leucogranites

6. Conclusions

The Bamenda granitoids is made up of two distinct types of granitic rocks (granites and leucogranites) displaying close field relationship. The differences between the two types are related to the sources and magma evolution within the crust. Both rocks have high K- calc-alkaline characters. Granites are of K-granitoids types whereas leucogranites are of Na-granitoids. These two groups of rocks are peraluminous with leucoganites more peraluminous and of S-type granite, while granites are slightly peraluminous and are of I-type. Granites show magnesian characters whereas leucogranites show ferriferous characters. Leucogranites are low Ba-Sr granitoids while granites are high Ba-Sr granitoids. The chondrite-normalized patterns show that the granites have higher concentrations of LREE than the leucogranites. In contrast their HREE concentrations are similar. The studied rocks show negative Eu anomaly. However, the Eu anomaly is strongly negative in leucogranites (Eu/Eu* = 0.23-0.36) and a weakly negative to null Eu anomalies (Eu/Eu* = 0.81-1.08) are observed in granites. Granites magma is derived from partial melting of metagreywackes whereas leucogranites magma resulted from partial melting of metapelites. The estimated temperatures of Bamenda granitoids magma range between 800°C and 950°C. Bamenda I-type granites are syn-tectonic and are similar to the other granitoids of the central domain of the Pan-African North-Equatorial Fold belt in Cameroon. Bamenda S-type peraluminous leucogranites are post-tectonic and chemically similar to the Himalayan peraluminous leucogranites. Furthermore decompression model may be related to Bamenda leucogranite formation. Tectonically the studied granitoids are related to crustal delamination characterizing the post-collisional event within the Pan African Fold Belt.

Acknowledgments

The authors are grateful to anonymous reviewers for their reviews and comments.

References

[1] Déruelle, B., Ngounouno, I. and Demaiffe, D., 2007. The “Cameroon Hot Line” (CHL): a unique example of active alkaline intraplate structure in both oceanic and continental lithospheres. Comptes Rendus Geoscience 339, 589-600.

[2] Gountié Dedzo, M., Nédélec, A., Nono, A., Njanko, T., Font, E., Kamgang, P., Njonfang, E. and Launeau, P., 2011. Magnetic fabrics of the Miocene ignimbrites from West-Cameroon: Implications for pyroclastic flow source and sedimentation. Journal of Volcanology and Geothermal Research 203, 113-132.

[3] Kamgang, P., Njonfang, E., Chazot ,G. and Tchoua, F. M., 2007. Géochimie et géochronologie des laves felsiques des Mounts Bamenda (ligne volcanique du Cameroun). Comptes Rendus Géoscience 339, 659-666.

[4] Nzenti, J. P., Kapajika, B., Wörner, G. and Lubala, R. T., 2006. Synkinematic emplacement of granitoids in a Pan-African shear zone in Central Cameroon. J. Afr. Earth Sci. 45, 74-86.

[5] Nzenti J. P., Abaga B., Suh C. E. and Nzolang C., 2011. Petrogenesis of peraluminous magmas from the Akum-Bamenda Massif, Pan-African Fold Belt, Cameroon. International Geology Review 53, 1121-1149.

[6] Kamgang, P., Chazot, G., Njonfang, E. and Tchoua, F. M., 2008. Geochemistry and geochronology of mafic rocks from Bamenda Mountains (Cameroon): Source composition and crustal contamination along the Cameroon Volcanic Line. Comptes Rendus Géoscience 340, 850-857.

[7] Nzenti, J. P., Barbey, P., Bertrand, J. M. and Macaudière, J., 1994. La chaîne panafricaine au Cameroun : cherchons suture et modèle!” In: S. G. F. (ed.), 15ème Réunion des Sciences de la Terre, Nancy, France, pp. 99.

[8] Ngnotué, T., Nzenti, J. P., Barbey, P. and Tchoua, F. M., 2000. The Ntui - Bétamba high-grade gneisses: a northward extension of the Pan- African Yaoundé gneisses in Cameroon. J. Afr. Earth Sci. 31, 369-381.

[9] Castaing, C., Feybesse, J.L., Thiéblemont, D., Triboulet, C. and Chèvremont, P., 1994. Paleo geographical reconstructions of the Pan-African/Brasiliano orogen: closure of an oceanic domain or intracontinental convergence between major blocks? Precambrian Research 69, 327-344.

[10] Neves, S.P., Bruguier, O., Vauchez, A., Bosch, D., Silva, J.M.R., 2006. Timing of crust formation, deposition of supracrustal sequences, and Transamazonian and Brasiliano metamorphism in the East Pernambuco belt (Borborema Province, NE Brazil): Implications for western Gondwana assembly. Precambrian Research 149, 197-216.

[11] Ganwa, A., Frisch, W., Siebel, W., Ekodeck, G.E., Cosmas, S. K. and Ngako, V., 2008. Archean inheritances in the pyroxene-amphibole-bearing gneiss of the Méiganga area (Central North Cameroon): Geochemical and $^{207}Pb/^{206}Pb$ age imprints. Comptes Rendus Geoscience 340, 211-222.

[12] Djouka-Fonkwé, M. L., Schulz, B., Schüssler, U., Tchouankoué, J. P. and Nzolang, C., 2008. Geochemistry of the Bafoussam Pan-African I- and S- type granitoids in western Cameroon. J. Afr. Earth Sci. 50, 148-167.

[13] Njiekak, G., Dörr, W., Tchouankoué, J. P. and Zulauf, G., 2008. U-Pb zircon and microfabric data of (meta) granitoids of western Cameroon: constraints on the timing of pluton emplacement and deformation in the Pan-African belt of Central Africa. Lithos 102, 460-477.

[14] Kouankap Nono, G.D., Nzenti, J.P., Suh Cheo, E., Ganno, S., 2010. Geochemistry of ferriferous, high-K calc-alkaline magmas from the Banefo-Mvoutsaha Massif (NE Bafoussam), Central Domain of the Pan-African Fold Belt, Cameroon. The Open Geology Journal 4, 15-28.

[15] Nzina Nchare, A., Nzenti, J.P., Tanko Njiosseu, E. L., Ganno, S. and Ngnotué, T., 2010. Synkinematic ferro-potassic magmatism from the Mekwene-Njimafofire Foumban Massif, along the Foumban-Banyo shear zone in central domain of Cameroon Pan-African fold belt. Journal of Geology and Mining Research 2(6), 142-158.

[16] Chebeu, C., Ngo Nlend, C.D. Nzenti, J-P., Ganno, S., 2011. Neoproterozoic high-K calc-alkaline granitoids from Bapa-Batié, North Equatorial Fold Belt, Central Cameroon: petrogenesis and geodynamic significance. The Open Geology Journal 5, 1-20.

[17] Middlemost, E. A. K., 1994. Naming material in the magma/igneous rock system. Earth-Science Review 37, 215–224.

[18] Peccerillo, A. & Taylor, S. R., 1976. Geochemistry of Eocene calc-alkaline volcanic rocks from the Kastamonu area, Northern Turkey. Contrib. Mineral. Petrol. 58, 63-81.

[19] Gills, J.B., 1981.Orogenic andesites and plates tectonics. Springer, Berlin.

[20] Hine, R., Williams, I. S. and Chappell, B. W., 1978. Contrasts between I- and S-type granitoids of the Kosciusko bathlith. *J. Geol. Soc. Australia* 25 (3), 219-234.

[21] Chappell, B. W. & White, A. J. R., 1992. I- and S-type granites in the Lachlan Fold Belt. Transactions of the Royal Society of Edinburgh: Earth Sciences 83, 1-12.

[22] Frost, B. R., Barnes, C. G., Collins, W. J., Arculus, R. J., Ellis, D. J. and Frost, C. D., 2001. A geochemical classification for granitic rocks. J. Petrol. 42, 2033-2048.

[23] Bertrand, J. M., Dupuy, C., Dostal, J. and Davidson, I., 1984. Geochemistry and geotectonic interpretation of granitoids from Central Iforas (Mali, West Africa). Precambrian Research 26, 265-283.

[24] Evensen, N. M., Hamilton, M. J. and O’Nions, R. J., 1978. Rare earth abundances in chondritic meteorites. Geochem. Cosmochim. Acta 42, 1199-1212.

[25] Hofmann, A.W., Jochum, K.P., Seufert, M., White, W.M., 1986. Nb and Pb in oceanic basalts: new constraints on mantle evolution. Earth and Planetary Science Letters 79, 33-45.

[26] Térakado, Y., & Masuda, A., 1988. Trace element variations in acidic rocks from the inner zone of southwest Japan. *Chem. Geol., 67*, 227-241.

[27] Kwékam. M., Hartmann, G., Njanko, T., Tcheumenak K. J., Fozing E. M., Njonfang, E., 2015. Geochemical and Isotope Sr-Nd Character of Dschang Biotite Granite: Implications for the Pan-African Continental Crust Evolution in West-Cameroon (Central Africa). Earth Science Research; 4, (1); 88-102

[28] Roberts, M. P. and Clemens, J. D., 1993. Origin of high-potassium, calcalkaline, I-type granitoids. Geology 21, 825-828.

[29] Shang, C. K., Satir, M., Nsifa, E. N.,Liegeois, J. P., Siebel, W. and Taubald, H., 2007. Archaean high-K granitoids produced by remelting of earlier Tonalite–Trondhjemite–Granodiorite (TTG) in the Sangmelima region of the Ntem Complex of the Congo craton, southern Cameroon. International Journal Earth Sciences 96, 817-841.

[30] Le Fort, P., Cuney, M., Deniel, C., France-Lanord, C., Sheppard, S. M. F., Upreti, B. N. and Vidal, P., 1987. Crustal generation of the Himalayan leucogranites. Tectonophysics, 134, 39-57.

[31] Guillot, S. and Le Fort P., 1995. Geochemical constraints on the bimodal origin of high Himalayan leucogranites. Lithos, 35, 221-234.

[32] Guo, Z., Wilson, M., 2012. The Himalayan leucogranites: Constraints on the nature of their crustal source region and geodynamic setting. Gondwana Research 22, 360–376.

[33] Watson, E.B. and Green, T.H., 1982. Apatite liquid-partition coefficients for the rare earth elements and strontium. Earth Planet. Sci. Lett. 56, 405-421.

[34] Watson, E.B. & Harrison, T.M., 1984. Accessory minerals and the geochemical evolution of crustal magmatic systems: a summary and prospectus of experimental approaches. Physics of Earth and Planetary Interiors 35, 19-30.

[35] Watson, E.B., 1987. The role of accessory minerals in granitoid geochemistry. In: Hutton Conference of the Origin of granites. Univ. Edinburgh, pp. 209-213.

[36] Liégeois, J. P., Abdelsalam, M. G., Ennih, N., and Ouabadi, A., 2013. Metacraton: Nature, genesis and behavior: Gondwana Research, v. 23, p. 220-237.

[37] Kwékam, M., Liégeois, J.P., Njonfang, E., Affaton, P., Hartmann, G., Tchoua, F., 2010. Nature, origin and significance of the Fomopéa Pan-African high-K calc-alkaline plutonic complex in the Central African fold belt (Cameroon). Journal African Sciences 54, 79–95.

[38] Kwékam, M., Affaton, P., Bruguier, O., Liégeois, J.P., Hartmann, G.,Njonfang, E.,2013. ThePan-African Kekem gabbro-norite (West-Cameroon), U–Pb zircon age, geochemistry and Sr–Ndisotopes: Geodynamical implication for the evolution of the Central African fold belt. Journal African Sciences 84, 70–88.

[39] Batchelor, R. A. & Bowden, P., 1985. Petrogenetic interpretation of granitoid rocks series using multicationic parameters. Chemical Geology 48, 43-55.

[40] Altherr, F. F., Holl, A., Hegner, E., Langer, C. and Kreuzer, H., 2000. High-potassium, calc-alkaline I-type plutonism in the European variscides: northern Vosges (France) and northern Schwarzwald (Germany). Lithos 50, 51-73.

[41] Liégeois, J. P., Black, R., Navez, J. and Latouche, L., 1994. Early and late pan African orogenies in the Aïr assembly of terranes (Tuareg Shield, Niger).Precambrian Research 67, 59-88.

[42] Liégeois, J.-P., Navez, J., Hertogen, J., Black, R., 1998. Contrasting origin of post collisional high-K calc-alkaline and shoshoniticversus alkaline and peralkalinegranitoids.The use of sliding normalization.Lithos 45, 1-28.